

Nanoparticle-Assisted Localized Optical Stimulation of Cultured Neurons

Flavie Lavoie-Cardinal, Charleen Salesse, Pierre-Luc Ayotte-Nadeau, and Paul De Koninck

Abstract

Nanoparticle-assisted localized optical stimulation (NALOS) of cultured neurons is an all-optical method that allows subcellular light stimulation to investigate localized signaling in neurons. The stimulation and monitoring of localized Ca^{2+} signaling in neurons takes advantage of plasmonic excitation of gold nanoparticles (AuNPs) with infrared light. In this chapter we describe how NALOS, through its effects localized to region smaller than $10\text{ }\mu\text{m}^2$, may be a useful complement to other light-dependent methods for controlling neuronal activity and cell signaling. We demonstrate that this technique can be applied to cultured hippocampal neurons using commercially available bare AuNPs.

Key words Photostimulation, Gold nanoparticles, Calcium imaging, Calcium signaling, Hippocampal neurons

1 Introduction

Light-induced stimulation of whole neurons or neuronal networks with optogenetic tools is a well-established and powerful approach to study circuit function [1]. With optogenetics, it is now possible to genetically control the subtype of neurons to be stimulated, to induce or inhibit neuronal activity, generally with a reduced level of invasiveness compared to electrical stimulation [2]. However, photostimulation at the nanometer to micrometer scale on neuronal membranes to investigate local signaling processes remains a challenge, primarily because light-gated channels have very small conductances. Neurotransmitter uncaging, with ultraviolet (UV) or two-photon excitation, has been used to precisely drive single synapse activation but is not optimal to activate a dendritic response at a nonsynaptic site [3]. It was shown recently that infrared (IR) short laser pulses can be used to excite neurons by affecting membrane capacitance, likely via a local heating process [4, 5]. This technique relies on the absorption of IR light by water and is

generally performed at wavelengths between 1400 and 2200 nm to better suit the absorption spectrum of water. It is very powerful for the stimulation of larger fields but sub-cellular stimulations are not possible since all cells in the excitation volume will be stimulated through the heating of the aqueous medium [4]. In this range of wavelengths, the coupling with standard UV to visible optics that can be used for confocal imaging is very difficult and limits considerably the confinement of the excitation spot to a diffraction limited region.

Taking advantage of their property to absorb visible and IR light, gold nanoparticles (AuNPs) and nanorods (AuNRs) have been used recently to generate light-induced heat for neuronal activation or inhibition [6–9]. Excitation of AuNPs with femtosecond laser pulses; near-field enhancement, or plasma generation was previously associated with nanocavitation formation and gene transfection [10–13]. Irradiation of 20 nm AuNPs by a 1 ms light pulse at 532 nm at a repetition rate of 40 Hz could be used to trigger action potentials (APs) [7], while prolonged IR illumination was associated with neuronal inhibition [8]. Through functionalization of the AuNPs, these techniques offer a higher specificity compared to the previously described IR water-mediated stimulation techniques. However, stimulation is limited to whole cells and requires a large number of AuNPs or AuNRs bound onto the cell [7, 9].

In this chapter we introduce a technique called Nanoparticle-Assisted Localized Optical Stimulation (NALOS) for localized, diffraction unlimited stimulation of subcellular regions on cultured hippocampal neurons by the mean of plasmonic excitation of a single AuNP [14]. For this technique, IR light at 800 nm is used for off-resonance plasmonic excitation of a targeted single AuNP. The evoked increased cellular activity is monitored by Ca^{2+} optical imaging and/or electrophysiology. The monitored subcellular increase in free Ca^{2+} concentration after the illumination of a single AuNP is confined to a few μm^2 . The elevation in free Ca^{2+} inside the neurons can also be widespread by raising laser intensity or the number of photostimulated NPs on the targeted cells. NALOS applied on large regions of interest (ROIs), containing more than one AuNP on the cell body, can be used to drive APs. On the other hand, NALOS applied on a dendritic compartment containing a single AuNP drives local and small currents capable of inducing localized Ca^{2+} responses. This technique does not require any genetic modification of the targeted cells, and binding of bare AuNPs onto the neuronal plasma membrane through passive sedimentation is sufficient. It is also possible to functionalize the AuNPs to target specific receptors on the membrane of the neurons [7, 9, 14, 15]. If the target receptor is cotransfected in the neuron (e.g., with a genetically encoded Ca^{2+} indicator), functionalization can help in restricting the binding of the AuNP

to the fluorescent neurons. However, stability of the functionalization during storage can be limiting.

NALOS can also be used to study local signaling downstream of Ca^{2+} , by monitoring for example the spatial and temporal dynamics of the Ca^{2+} /calmodulin-dependent kinase (CaMKII) tagged with GFP in combination with Ca^{2+} imaging using a red calcium sensitive protein such as RGCaMP1.07 or NES-jRGECO1 [14]. In this configuration, two-color confocal imaging combined with infrared optical stimulation, without measurable cross talk between the three channels, is possible on most commercial confocal microscopes equipped with a two-photon excitation path. Electrophysiological recordings can also be performed simultaneously in order to characterize the membrane currents evoked by the photostimulation.

2 Materials

2.1 Gold Nanoparticles

The choice of the AuNP particle size is of great importance for NALOS, since it influences strongly the required laser intensity and the observed effect on the targeted neurons. Increasing the AuNP size generally increases light absorbance and induces a red shift of the plasmonic absorbance band, thereby increasing the amplitude of the cell response and the risks of membrane damages. On the other hand, larger AuNPs allow considerable reduction of the infrared light intensity required for photostimulation.

When suspending AuNPs in physiological media, their aggregation has to be monitored. It is important to recognize aggregates and only illuminate single AuNPs, for better reproducibility. In our hands, smaller nonfunctionalized AuNPs tend to agglomerate more easily in the culture media used compared to larger ones; we therefore favor 100 nm AuNPs.

An important consideration in the choice of the NPs is their absorption at the available wavelengths and intensities of the confocal system in hand, which needs to be compatible with the imaging application. Increasing the AuNP diameter leads to a shift to longer wavelengths of the surface plasmon absorbance (from 520 to 580 nm for 20–80 nm AuNPs) and therefore decreases the required laser intensity for an IR off-resonance plasmonic excitation [16, 17].

If the AuNPs need to be localized precisely on the cell membrane using their light scattering properties, as it is the case for NALOS, their size will also influence the required laser intensity and the choice of the wavelength [16]. With increasing AuNP size the scattering spectrum is shifted to longer wavelengths and the scattering efficiency at 600 nm is also increased [16]. We could detect easily 100 nm single AuNPs with their scattering at 633 nm,

while when using 20 nm AuNPs we could detect only aggregates at this wavelength.

In our experience, AuNPs of 100 nm diameter are very good for localized photostimulation with IR light as well as their localization with red light (633 nm). This size of AuNPs enables the use of IR laser intensity well below (~ 1 order of magnitude) that necessary for two-photon excitation [18]. Meanwhile, 488 and 543 nm excitation (intensity below 5 μW in the back aperture of the objective) does not generate sufficient absorption by the AuNPs to cause a detectable cellular response.

2.2 Rat Hippocampal Cultures and Transfections

For the primary rat hippocampal cultures, neonatal rats of 0–2 days old were used. The dissociated cells were plated on 12 mm poly-D-lysine-coated glass coverslips at a density of 4225 cells/ mm^2 . Growth media consisted of Neurobasal and B27 (50:1), supplemented with penicillin/streptomycin (50 U/mL; 50 $\mu\text{g}/\text{mL}$) and 0.5 mM Glutamax (Invitrogen). Fetal bovine serum (2%; Hyclone) was added at time of plating. After 5 days, half of the media was replaced by media without serum and with Ara-C (5 μM ; Sigma-Aldrich) to limit proliferation of nonneuronal cells. Twice a week thereon, half of the growth media was replaced with media free of serum and Ara-C. The neurons were transfected at 11–14 days in vitro and imaged 1 day after transfection.

For the transfection half of the culture media was taken out of the wells and mixed in new wells with the same amount of fresh complete growth media. The transfection was performed in the remaining media (500 μL in the case of a 24 well plate and 12 mm coverslips). For 12 mm coverslips, 0.5 μg DNA and 2 μL Lipofectamine 2000 (Invitrogen) were mixed in 100 μL Neurobasal media and added dropwise on the cells. After 3–5 h, the coverslips were transferred in the new wells containing 50/50 fresh/old growth media.

For Ca^{2+} imaging, plasmids encoding GCaMP6s [19], NES-jRGECO1 [20], or RCaMP1.07 (gift of J. Nakai) were used. Alternatively, transfections can be substituted by the incubation with cell-permeable Ca^{2+} -sensitive dyes, such as Fluo4-AM (2 μM , 30 min incubation, 30 min wash). For electrophysiology measurements, the Ca^{2+} -sensitive dye can also be loaded through the patch pipette (Fluo4, 337 nM).

2.3 Experimental Setup

NALOS can be performed on any commercial or custom-built confocal microscope. In our experiments, we used a confocal laser scanning microscope (Zeiss, LSM 510) equipped with an 80 MHz pulsed femtosecond infrared laser (Ti:Sapphire, Chameleon, Coherent). To perform photostimulation and Ca^{2+} imaging, the microscope should be equipped with both IR and visible excitation paths.

Fluorescence excitation of GCaMP6s or mGFP was performed with a 488 nm continuous wave (cw) laser (intensity in the back aperture of the objective below 5 μW) and detected using an

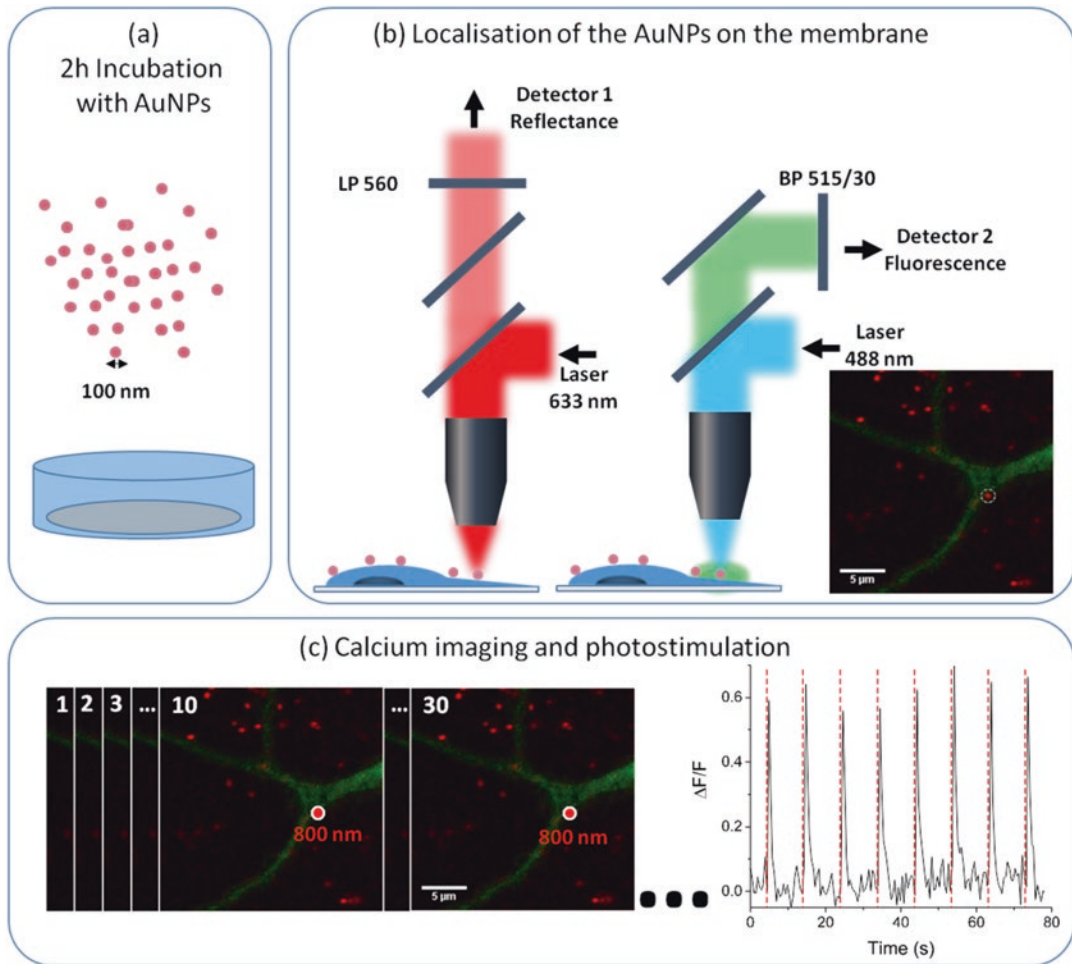


Fig. 1 Experimental procedure. (a) Incubation with 100 nm AuNPs for 2 h directly in the well plates. (b) Localization of the AuNPs on the cellular membrane in reflectance at 633 nm (red) combined with fluorescence microscopy of neurons transfected with GCaMP6s (green). (c) Time lapse imaging and photostimulation of the ROI marked with the white circle and $\Delta F/F$ signal quantified in the same ROI (dotted lines indicate times of photostimulation)

IR-blocking 500–550 nm filter (Fig. 1b). Fluorescence excitation of RCaMP1.07, NES-jRGECO, or mCherry was done with 543 nm cw laser (intensity in the back aperture of the objective below 5 μ W) using an IR-blocking 565–615 nm filter. Visualization of the AuNP reflection was done with a 633 nm cw laser (laser power in the back aperture of the objective below 500 nW) and a 560 nm long pass fluorescence filter (Fig. 1b). Live-cell imaging was performed with an open perfusion chamber and a 40 \times 0.8NA water dipping objective.

For the photostimulation, we used a Ti-Sapphire laser at 800 nm; its power in the back aperture of the objective was tuned between 0.5 and 2 mW (0.27–1.02 MW/cm²). For NALOS, a single scan

over a ROI was performed with a pixel dwell time varying between 1.3 and 6.4 μs . In order to monitor simultaneously the AuNP positions and the cellular activity with Ca^{2+} imaging, the microscope should be equipped with at least two independent detection paths.

It is important to consider that the plasmon absorbance maximum of AuNPs is in the visible range of the spectrum and that the laser intensity used for confocal imaging should be below the threshold necessary for plasmonic excitation. In our experience, the excitation of the fluorescent proteins in the visible range with a cw laser at the imaging intensity of 0.2–0.9 kW/cm^2 had no measurable effect on the neurons in contact with AuNPs.

Since a femtosecond pulsed IR laser at 800 nm is used for off-resonance plasmonic excitation of the AuNPs, it needs to be tuned to intensities that are below the ones needed for two-photon excitation of the chosen fluorescent marker. Green fluorescent markers show typically a good two-photon absorption between 800 and 920 nm and therefore the laser power in the back aperture of the stimulation beam was kept below 2 mW (1.02 MW/cm^2), which was on our setup about one order of magnitude below the lower threshold of two-photon excitation of the fluorescent markers used. This need to be tuned depending on the microscope objective and the fluorescent probes used.

2.4 Optical Imaging Solution

Neurons were imaged in an open chamber in HEPES-aCSF (in mM: 102 NaCl, 5 KCl, 10 HEPES, 1.2 CaCl_2 , 1 MgCl_2 , 10 $\text{C}_6\text{H}_{12}\text{O}_6$, pH 7.4, 230–240 mOsm) using a perfusion system with temperature adjusted to 29–30 $^{\circ}\text{C}$. The osmolarity of the HEPES-aCSF solution needs to be adjusted as close as possible to the osmolarity of the culture media. In our experiments, the osmolarity was adjusted between 230 and 240 mOsm (similar to Neurobasal). For electrophysiology experiments, 0.5 μM tetrodotoxin (TTX) was added to the imaging solution.

2.5 Intracellular Solutions for Patch Clamp Recordings

For patch clamp recordings in current clamp mode, the solution consisted of (in mM) 111 KMeSO_3 , 10 diNa-phosphocreatine, 10 HEPES, 2.5 MgCl_2 , 2 ATP-Tris, 0.4 GTP-TRIS, at pH 7.25–7.35; the osmolarity was adjusted to 210–220 mOsm/L. For patch clamp recordings in voltage clamp mode, the solution consisted of (in mM) 96 CsMeSO_3 , 20 CsCl , 10 diNa-phosphocreatine, 10 HEPES, 2.5 MgCl_2 , 0.6 EGTA, 4 ATP-TRIS, 0.4 mMGTP-TRIS, at pH 7.25–7.35; the osmolarity was adjusted 210–220 mOsm/L.

3 Methods

3.1 Incubation with AuNPs

Prior to imaging, incubation for 2 h of the AuNPs onto the neurons inside the incubator allowed for sufficient sedimentation (Fig. 1a). Fifty microliters of the stock solution (50 $\mu\text{g}/\text{mL}$, 100 nm

diameter, Nanopartz, A11-100-CIT-100, 5.71×10^9 AuNPs/mL, $\epsilon = 1.1 \times 10^{11} \text{ M}^{-1} \text{ cm}^{-1}$, potential zeta -46 mV) was mixed with $50 \mu\text{L}$ of Neurobasal culture media and added dropwise to the cells in 1 mL growth media. The optimal ratio between the mixed AuNPs-Neurobasal solution and the growth media in the well was 1:10. This incubation protocol yielded between 20 and 40 detectable AuNPs in an area of $40 \times 40 \mu\text{m}$. Longer incubation times or higher AuNP concentration increased the probability of AuNP aggregation. After incubation, no washing step was necessary; the coverslip with neurons in contact with AuNPs could be transferred directly to the imaging chamber.

3.2 Nanoparticle-Assisted Local Optical Stimulation

First, a fluorescence image of a neuron expressing a Ca^{2+} indicator and a reflection image of the AuNPs were taken and overlaid (Fig. 1b). AuNPs that appear in contact with a dendrite of the transfected neuron were then identified. To avoid AuNP aggregates, only AuNPs showing a diffraction limited point spread function were chosen for photostimulation. Since the scattering of the AuNPs is shifted to longer wavelengths upon agglomeration, the intensity of the reflection PSFs of AuNPs at 543 and 633 nm can also be compared. Indeed, the monomers should show a stronger reflection at 543 nm, while clusters will reflect more at 633 nm.

The photostimulation step was performed using the ROI-bleaching module of the LSM-510 Zeiss microscope. ROIs of $1\text{--}10 \mu\text{m}^2$ were chosen around an AuNP for the IR-photostimulation (Fig. 1c). A single scan over a ROI was sufficient to induce a measurable local Ca^{2+} response. Increasing the number of scans over a ROI (up to ten iterations) can be used to increase the probability of successful stimulation at low laser intensity.

Using the ROI-bleaching module of the LSM510 microscope, a series of ten images were taken prior to stimulation. The IR-illumination was then performed for a given number of iterations (generally between 1 and 5) on the ROI and imaging was carried on for the desired lapse of time. Repeated photostimulation on the same AuNP was possible, while monitoring its movement via the reflection images (Fig. 1c).

Laser power below 2 mW at the back aperture of the objective was required to induce a reversible widespread Ca^{2+} response, while less than 1 mW was preferable to induce a local and reversible response [14]. At this power, no cross talk between stimulation and fluorescence excitation was observed. Higher illumination intensities lead to irreversible Ca^{2+} response suggesting damages of the plasma membrane.

3.3 Calcium Imaging

Optical imaging of Ca^{2+} can be performed alone or in combination with a second fluorescent signal, such as CaMKII tagged with a fluorescent protein (Fig. 1c). The scanning speed and size of the imaged region were adjusted to obtain sufficient temporal

resolution of the Ca^{2+} signals, according to the kinetics of the chosen indicator. The pixel size was adjusted to fulfill the Nyquist criterion and the pixel dwell time varied between 1.3 and 6.4 μs . Ca^{2+} indicators with slow kinetics and bright fluorescence, such as GCaMP6s, NES-JRGECO1, and RCaMP1.07, were chosen to obtain a sufficient signal to noise ratio even for a local Ca^{2+} response confined to a few μm^2 . Imaging rates between 2 and 4 Hz were sufficient.

The fluorescence intensity over a chosen ROI was averaged and subtracted with the averaged background intensity. The obtained fluorescence intensity (F) was corrected by the mean average intensity in this region in the ten imaged frames before stimulation (F_0) to obtain the corrected $\Delta F/F_0$ traces (Fig. 1c).

3.4 Electro-physiological Recordings

As described in Fig. 2a, we identified a fluorescent neuron that had dendrites with overlapping AuNPs, using fluorescence imaging and reflectance. For recordings, a glass pipette with a resistance of 3.5–5 $\text{M}\Omega$ was filled with intracellular solution. Alternatively, a Ca^{2+} sensitive dye such as Fluo4 could be added to the intracellular solution for recordings on nontransfected cells. Low positive pressure was applied in the pipette while in the bath, and was released upon touching a neuronal cell body, which could be seen by a slight deflection of the membrane, visually identified using a 40 \times water-immersion objective and infrared differential interference contrast (Zeiss Axioscop FS2). Negative pressure was then applied until resistance reached at least 1 $\text{G}\Omega$. Pipette capacitance was automatically adjusted by the software before breaking the seal and achieving whole-cell configuration. Cell health, monitored throughout the experiment, was established by stable holding

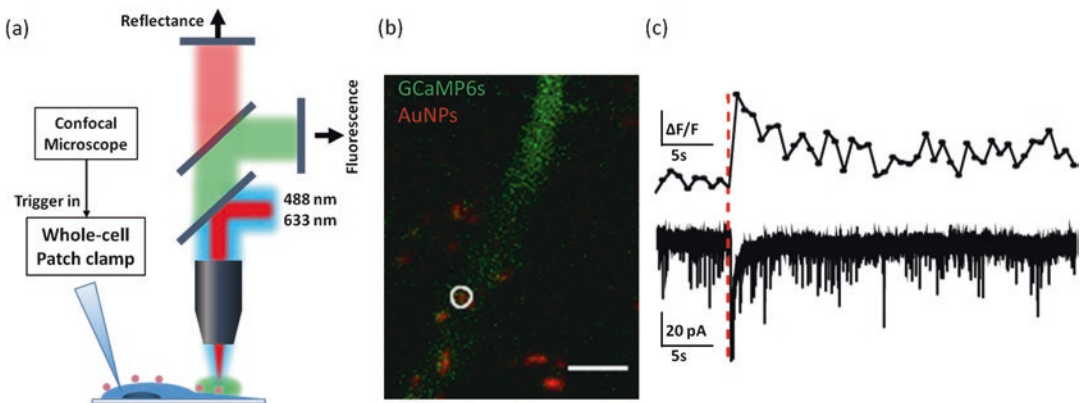


Fig. 2 Simultaneous electrophysiological and optical recordings. **(a)** Simultaneous electrophysiological and optical recording combined with photostimulation. The electrophysiological recording was triggered by the LSM510 microscope to ensure synchronization of both traces. **(b)** Ca^{2+} imaging (GCaMP6s fluorescence, green) after AuNP localization (reflectance, red); scale bar 5 μm . **(c)** Ca^{2+} signal (upper trace) is correlated to the corresponding electrophysiological trace (lower trace)

current and series resistance: $\alpha \pm 20\%$ change was tolerated. Data acquisition (filtered at 1.8–2 kHz and digitized at 10 kHz) was performed using a Multiclamp 700B amplifier and the Clampex 10.6 software (Molecular Devices). The electrophysiological recordings were triggered by the LSM510 confocal microscope for synchronization with the Ca^{2+} imaging (Fig. 2a, b). Data were analyzed using Clampfit 10.6 (Molecular Devices) and Igor Pro (WaveMetrics).

References

1. Fenno L, Yizhar O, Deisseroth K (2011) The development and application of optogenetics. *Annu Rev Neurosci* 34:389–412
2. Deisseroth K (2011) Optogenetics. *Nat Methods* 8:26–29
3. Matsuzaki M, Ellis-Davies GC, Nemoto T et al (2001) Dendritic spine geometry is critical for AMPA receptor expression in hippocampal CA1 pyramidal neurons. *Nat Neurosci* 4:1086–1092
4. Shapiro MG, Homma K, Villarreal S et al (2012) Infrared light excites cells by changing their electrical capacitance. *Nat Commun* 3:736
5. Wells J, Kao C, Mariappan K et al (2005) Optical stimulation of neural tissue in vivo. *Opt Lett* 30:504–506
6. Eom K, Kim J, Choi JM et al (2014) Enhanced infrared neural stimulation using localized surface plasmon resonance of gold nanorods. *Small* 10:3853–3857
7. Carvalho-de-Souza JL, Treger JS, Dang B et al (2015) Photosensitivity of neurons enabled by cell-targeted gold nanoparticles. *Neuron* 86:207–217
8. Yoo S, Hong S, Choi Y et al (2014) Photothermal inhibition of neural activity with near-infrared-sensitive nanotransducers. *ACS Nano* 8:8040–8049
9. Nakatsuji H, Numata T, Morone N et al (2015) Thermosensitive ion channel activation in single neuronal cells by using surface-engineered plasmonic nanoparticles. *Angew Chem Int Ed* 54:11725–11729
10. Schomaker M, Heinemann D, Kalies S et al (2015) Characterization of nanoparticle mediated laser transfection by femtosecond laser pulses for applications in molecular medicine. *J Nanobiotechnol* 13:10
11. Baumgart J, Humbert L, Boulais É et al (2012) Off-resonance plasmonic enhanced femtosecond laser optoporation and transfection of cancer cells. *Biomaterials* 33:2345–2350
12. Boulais É, Lachaine R, Meunier M (2012) Plasma mediated off-resonance plasmonic enhanced ultrafast laser-induced nanocavitation. *Nano Lett* 12:4763–4769
13. Schomaker M, Killian D, Willenbrock S et al (2015) Biophysical effects in off-resonant gold nanoparticle mediated (GNOME) laser transfection of cell lines, primary- and stem cells using fs laser pulses. *J Biophotonics* 8:646–658
14. Lavoie-Cardinal F, Salesse C, Bergeron É et al (2016) Gold nanoparticle-assisted all optical localized stimulation and monitoring of Ca^{2+} signaling in neurons. *Sci Rep* 6:20619
15. Bergeron E, Boutopoulos C, Martel R et al (2015) Cell-specific optoporation with near-infrared ultrafast laser and functionalized gold nanoparticles. *Nanoscale* 7:17836–17847
16. Jain PK, Lee KS, El-Sayed IH et al (2006) Calculated absorption and scattering properties of gold nanoparticles of different size, shape, and composition: applications in biological imaging and biomedicine. *J Phys Chem B* 110:7238–7248
17. Link S, El-Sayed MA (2010) Shape and size dependence of radiative, non-radiative and photothermal properties of gold nanocrystals. *Int Rev Phys Chem* 19:409–453
18. Mütze J, Iyer V, MacKlin JJ et al (2012) Excitation spectra and brightness optimization of two-photon excited probes. *Biophys J* 102:934–944
19. Chen T-W, Wardill TJ, Sun Y et al (2013) Ultrasensitive fluorescent proteins for imaging neuronal activity. *Nature* 499:295–300
20. Dana H, Mohar B, Sun Y et al (2016) Sensitive red protein calcium indicators for imaging neural activity. *Elife* 5:pil: e12727

Use of Nanoparticles in Neuroscience

Santamaria, F.; Peralta, X. (Eds.)

2018, XVI, 296 p. 98 illus., 66 illus. in color., Hardcover

ISBN: 978-1-4939-7582-2

A product of Humana Press